INTERNATIONAL JOURNAL OF MARITIME TECHNOLOGY
IJMT Vol.15/ Winter 2021 (67-78)
Available online at: www. ijmt.ir

Post Buckling Analysis with Different Configurations of Snaked Laid Pipelines

Yasaman Rezaie[1], Seyed Mohammad Hossein Sharifi[2*], Gholam Reza Rashed[3]

[1] *M. Sc in Mechanical Engineering, Petroleum University of technology; yasaman.rezaie@afp.put.ac.ir*
[2*] *Assistant Professor of Mechanical Engineering Department, Petroleum University of Technology; sharifi@put.ac.ir*
[3] *Associated Professor of Mechanical Engineering Department, Petroleum University of Technology; g.rashed@put.ac.ir*

ARTICLE INFO

Article History:
Received: 28 Mar. 2021
Accepted: 29 Jun. 2021

Keywords:
Offshore Pipelines
Snake Lay Configuration
High Pressure/ High Temperature
Global Buckling Failure
Lateral Buckling

ABSTRACT

A common solution for oil and gas transportation in offshore fields is long distance pipelines. Flowing of High Pressure/ High Temperature (HP/HT) fluid may cause uncontrolled buckling because of material or geometry defects. In order to reduce damages and avoid buckling in unpredictable places, the controlled buckling concept is introduced. In order to trigger buckling in predetermined location, pipeline can be placed in snaked lay configuration. In this article, it is aimed to investigate the effect of geometrical parameters, i.e., laying wavelength, laying radius and offset angle of snaked lay configuration on the displacement of offshore pipelines, axial force and bending moment in post buckling stage under HP/HT condition. Then, these results are used to evaluate the global buckling failure. This work is performed by using nonlinear finite element analysis and pipe-soil interaction of as-laid pipelines is modeled by employing spring elements. The results of investigation show that different ranges of the mentioned parameters may cause the maximum difference in displacement, bending moment and axial force about 133.6%, 155%, and 30%, respectively. Investigation of global buckling failure determine the most critical section of pipelines and it is observed that as the curved section of pipeline shrinks, the possibility of global buckling failure will increase but the effect of laying wavelength is contrary and the failure will be decreased about 8.3%.

1. Introduction

Since 1970's, submarine pipelines gradually become the main way in offshore engineering to transport oil and gas all over the world [1]. Generally speaking, higher pressure and temperature of the flowing fluid in pipes lead to facilitation of the flow and decrease chance of precipitation of asphaltene and wax components. On the other hand, these operation conditions may cause thermal expansion in axial direction of pipe. These expansions could be limited by pipe-soil interactions or end connections of the pipes which kept the pipelines in position. As a result, axial stresses are created that can cause pipeline buckling [2]. Buckling is a side way deflection that is caused by increasing the applied load. When this load becomes large enough to make a member unstable, then it is said to have buckled. According to DNV-RP-F110 [3], there are three different scenarios of operational conditions of HP/HT pipelines:

1. Uncovered pipelines on the flat and smooth seabed which experience global buckling in the horizontal plane;
2. Uncovered pipelines on the un-even seabed which experience, at first, global deformation in the vertical plane and subsequently in horizontal plane;
3. Covered pipelines which experience upheaval buckling. This kind of global buckling happens in the vertical plane.

There are two different methods to prevent inappropriate effects of lateral buckling: (a) totally constrained method, and (b) controlled lateral buckling concept. In the first suggested method, pipeline movement is constraint in any direction which is possible by techniques such as trenching, burying and rock dumping, but these solutions are not economical. In contrast, in second method, it is proposed to work

with pipeline rather than operating against it, i.e. lateral buckling is triggered at a number of predetermined locations in order to prevent severe buckles occurring at a few random sites [4]. Comparing both methods shows that the second method is more cost effective. Some of the methods used in practice to control the number of buckles are terrain irregularities, vertical triggers, buckle initiation using distributed buoyancy or additional insulation coating and snake lay which are described in more details in [4]. The possibility of buckle formation at these controlled locations will be increased through introducing out-of-straightness (OOS) features or reduction of lateral soil resistance [5].

Studies of pipeline global buckling started with the work of Hobbs [6] that investigated lateral and vertical buckling of an ideal offshore pipeline. In his study, the effects of the friction coefficient and the various lateral modes are considered on pipeline global buckling behavior and the introduced solution represented the classical analytical solution for perfect pipelines. Taylor and Gan [7] presented analytical solutions for lateral global buckling modes I and II which are uncovered submarine pipelines with two primary initial imperfections. Thereafter, a lot of theoretical analyses in lateral buckling have been introduced which are based on Hobbs Work. An analytical solution for high order lateral buckling modes of offshore pipelines are suggested by Hong et al. [8] which have one symmetric imperfection. Tianfeng and Xianhong [9] introduced an analytical solution for buckling analysis of offshore pipelines that were restrained by two segmented ditching constructions. The lateral buckling response of offshore pipelines that were triggered by one sleeper was investigated by Wang et al.[10] and an analytical solution was proposed for this case. Wang et al. [11, 12] studied lateral buckling which are triggered by distributed buoyancy section and introduced some analytical solutions for the case. Other works were performed by Wang et al. [13], Shi et al. [14], and Shi and Wang [15]. Due to different simplifying assumptions, analytical solutions have inherent limitations in research on buckle initiation and post buckling investigations. With the development of numerical simulation tools, the simulation of pipeline lateral global buckling under complex conditions could be carried out. The simulation methods, different types of boundary conditions and loading, pipe-soil interaction and other key parameters such as pipeline section dimension and imperfection geometry were discussed for better modeling results and investigation their influences on the deformation and stress distribution.

The snake laying method is the most economical compared to the other suggested means. The main difference between this method and the vertical trigger is that there are no resulting spans and consequently no vortex-induced vibrations (VIV) or trawl hooking loads [16]. To understand the benefits of the snake laying method, Li et al. [17], Liu et al. [18], and Jiang Gung et al. [19] have compared various studies to reveal the advantages of this technique.

There are some successful projects, e.g. the Penguins project [20] and the Echo Yodel project [21] in which the snaked laying method has been used in practice. Preston et al. [22] presented a summary of accepted methodology and performed some analyses to specify an acceptable as-laid pipeline geometry. Rundsag et al. [4] and Rathbone et al.[23] implemented a parametric study to evaluate the effect of snake lay geometry on the buckle initiation force, resulting bending moment, and strain by the finite element (FE) software ABAQUS. The investigated parameters included lay radius, arc length, and offset angle. Cumming and Rathbone [24] studied the relationship between the minimum buckle initiation force and the horizontal offset angle of a pipeline, considering an Euler buckling approach. In the end, a relationship is proposed that estimates the buckle initiation force based on pipeline stiffness and weight, offset angle, and friction factor which is then compared against idealized finite element models. Obele Ifena [25] studied the influence of pipe-soil interaction on the design of surface laid subsea pipelines susceptible to lateral buckling. Rezaie et al. [26] investigated the effect of HP/HT loading and section dimensions on critical buckling force by considering internal pressure. Liu et al. [27] suggested a new configuration for curved section of snaked laying method. It is recommended to use a sinusoidal configuration instead of circular sections which can reduce the buckle initiation force. Wang et al. [16] proposed a new shape of snaked laying curve based on a combination of genetic algorithm (GA) and finite element analysis. A summary of reviewed literature is introduced in Figure 1.

All the studies mentioned above have addressed pipelines that experienced high temperatures, but they have overlooked the effect of external and internal pressures. More specifically, the effect of the pressure difference has been converted into an equivalent temperature difference, as explained in more detail in [8, 28]. Besides, most parametric studies in this field have focused on the buckle initiation and investigation of effective parameters on the buckle initiation force. So, the present study focuses on the assessment of displacement, axial force and bending moment of submarine pipeline in the post buckling condition by considering the effects of laying radius, offset angle and wavelength of snaked laid pipeline. In the next step, the introduced relationships of DNV-OS-F101

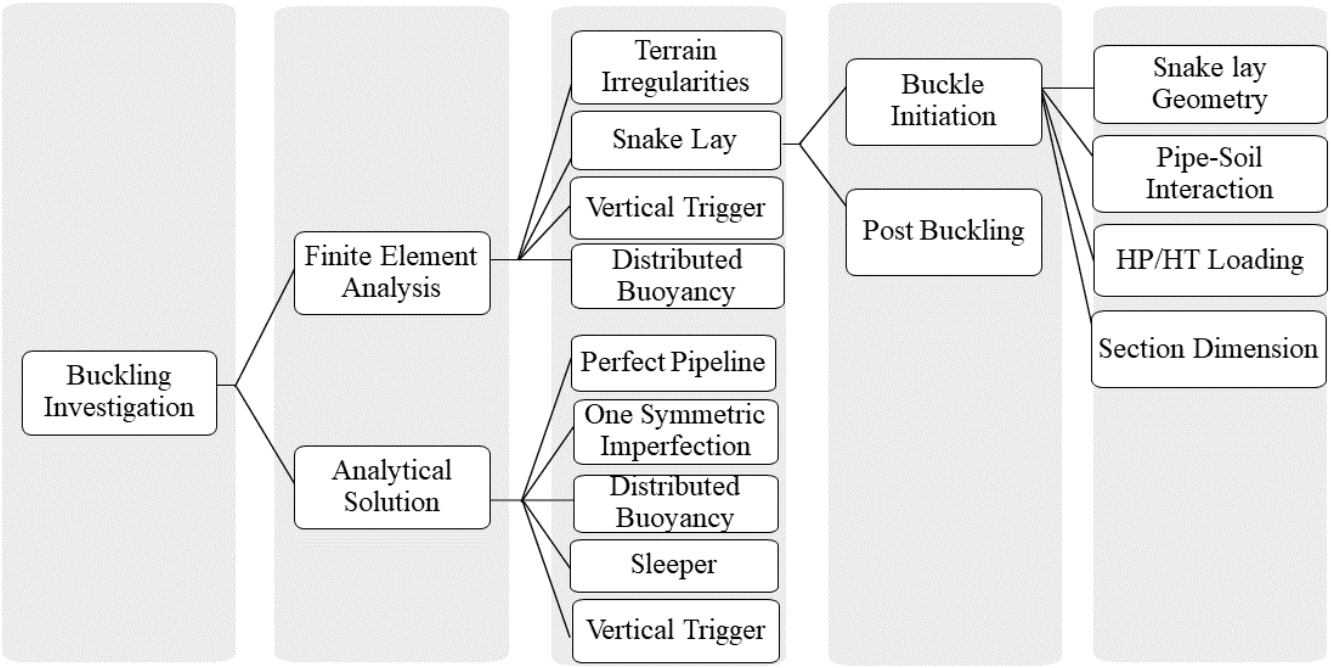

Figure 1. Review of literature

[29] in stress based are used to investigate the failure of pipeline because of global buckling.

2. Finite Element Modeling

2.1. Configuration of Snaked Lay Pipelines

A typical configuration of snaked-lay pipelines composed of a straight section and a curved section is shown in Figure 2. The straight section is usually longer than the curve one and it can be described by L, V and β called laying wavelength, amplitude curvature, and laying chord length, respectively. In this figure, "ab", "de", "ef", and "hi" are examples of the straight section. The configuration of a typical arc curve section is described in more detail in which the lay radius R and the offset angle θ control the shape of the curved section. Examples of the curved section include "bcd" and "fgh". It is significant to know that the relationship between the lay radius, offset angle, and laying chord length can be expressed by Eq. (1):

$$\beta = R \times \theta \quad (1)$$

Because of symmetric loading and geometry, just a quarter of pipeline length is simulated in Figure 2, i.e. "cde". In this article, a pipeline with outer diameter and thickness of 182 mm and 16.2m m is considered.

2.2. Pipeline Properties

The inputs for material properties include basic data such as Young's modulus, Poisson's ratio, thermal expansion coefficient, and yield strength, which are listed in Table 1. The carbon steel material used for the pipe is API 5L grade X65.

Table 1. The material properties of pipeline [30]

Characteristic	Value
Elasticity modulus (E_{steel})	2.07×10^{11} [$N\ m^{-2}$]
Poisson's ratio (ν)	0.3 [-]
Thermal expansion coefficient (α)	1.1×10^{-5} [$℃^{-1}$]
Yield stress	545 [Mpa]
Density (ρ)	**7850** [$\frac{kg}{m^3}$]

The isotropic power law is adopted to describe the pipeline material behavior as expressed in more detail by Eq. (2):

$$\sigma = \begin{cases} E\varepsilon & \varepsilon \le \varepsilon_y \\ \sigma_0 (\frac{\varepsilon}{\varepsilon_y})^n & \varepsilon > \varepsilon_y \end{cases} \quad (2)$$

Where σ_0 is the yield stress, n is the strain hardening assumed to be 0.05 and ε_y is the yield strain, which is equal to 0.00263. 3-D finite element simulations were performed using ABAQUS standard code [31]. The pipe was modeled using eight-node 3D elements (C3D8R).

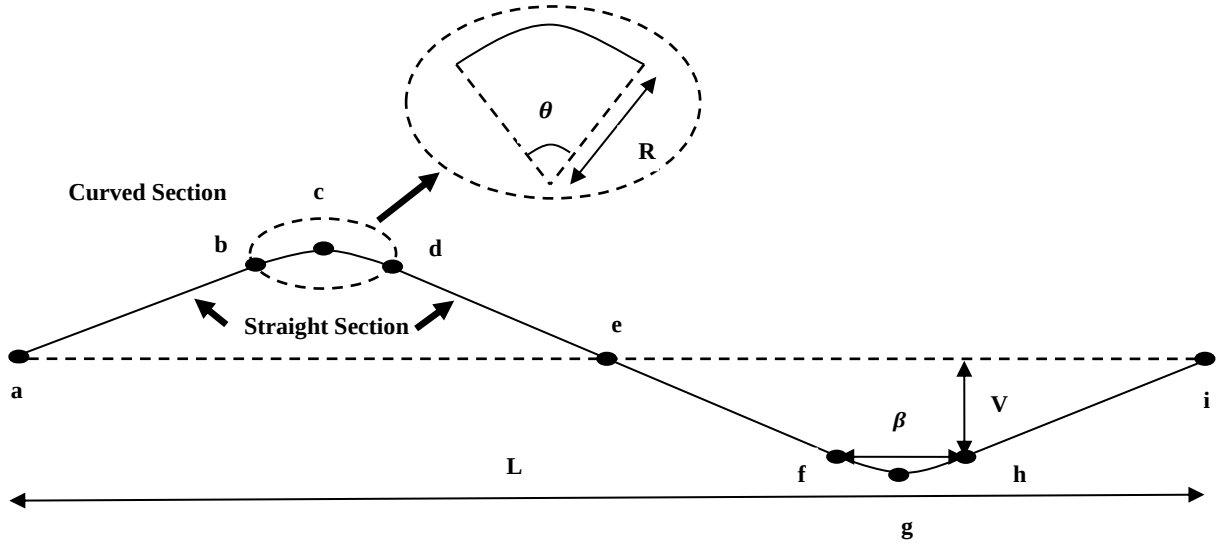

Figure 2. Snake lay configuration [26]

2.3. Pipe-Soil Interaction

In this research, submerged weight is considered. The presence of this loading introduces self-weight on each SPRING1 elements in order to consider axial, lateral and normal interactions as shown in Figure 3.

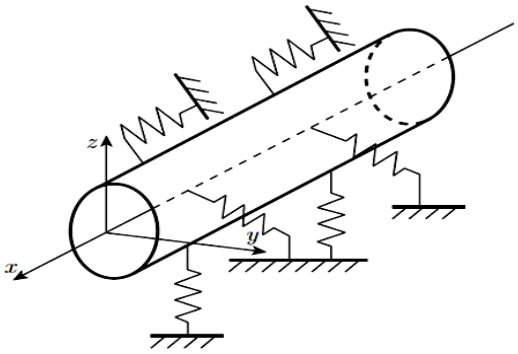

Figure 3. The pipe-soil interaction model by using SPRING elements [27]

SPRING1 is placed between the seabed and outer pipe nodes and acts in a fixed determined direction. Bi-linear and tri-linear resistance models are selected for axial and lateral pipe-soil interactions, respectively. For normal interaction, it is assumed that the spring has high values of stiffness in order to prevent the motion of the pipeline in this direction. The basic parameters for the description of resistance models are listed in Table 2.

element of the pipeline and consequently creates an interaction between pipeline and soil. The simulation of this contact can be performed by using

Table 2. The basic parameters for the pipe-soil interaction [23]

Characteristic	Value
Axial break out displacement	10 $[mm]$
Axial friction coefficient	0.6 [-]
Lateral break out displacement	140 $[mm]$
Peak lateral friction coefficient	1.1 [-]
Residual lateral displacement	990 $[\boldsymbol{mm}]$
Residual lateral friction coefficient	0.6 [-]

2.4. Pipeline Loading

A 3D model is used to simulate the pipeline global buckling behavior. Disregarding the wave-current load and residual lay tension associated with the installation, five main forces act on a pipeline including hydrostatic pressure, the submerged weight of the pipeline, internal pressure, soil resistance, and temperature load [32]. In this investigation, loading is constant and the values of temperature and internal pressure is assumed about 90℃ and 1.2 MPa. The boundary conditions of the pipeline are shown in Figure 4. Because of pipeline configurations, some residual strain will be created in pipeline which is not considered in this paper.

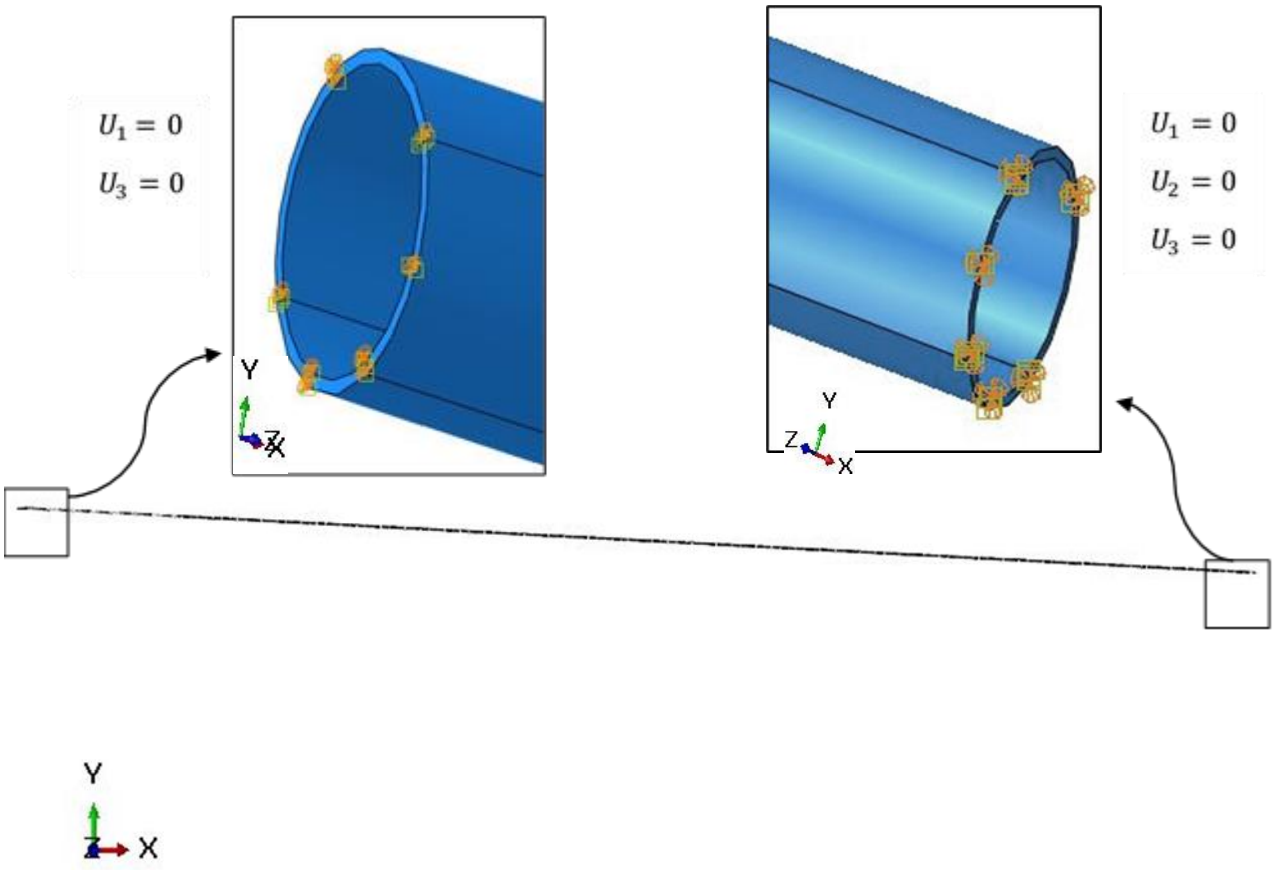

Figure 4. Boundary conditions of one-quarter of pipeline

3. Global Buckling Failure Assessment Coefficient

According to DNV-OS-F101[29], the global buckling failure in post-buckling stage of pipeline can be evaluated by determining either the maximum internal force combination or the maximum compressive strain. So, the methods of assessment can be categorized to (a) Load Control Combination and (b) Displacement Control Combination, which first is based on maximum internal force combination and second is based on maximum compressive strain. Since the Load Control Criterion is stricter; therefore, it has been selected as an evaluation criterion in this paper. The assessment judgement formula for the Load Control Condition is:

$$\left(\gamma_m\gamma_{SC}\frac{M}{\alpha_c M_p}+\left(\frac{\gamma_m\gamma_{SC}P}{\alpha_c S_p}\right)^2\right)^2+\left(\alpha_p\frac{p_i-p_e}{\alpha_c p_b}\right)^2\leq 1 \quad (3)$$

Where $\gamma_m$is the material resistance factor of pipeline, γ_{SC} is the safety class resistance factor, α_c is the flow stress parameter, M is the bending moment of the deformed pipeline cross-section, M_p is the equivalent yield bending moment, P is the axial force of deformed pipeline cross-section, S_p is the equivalent yield axial force, α_p is the section size coefficient and p_b is the burst pressure. By assuming θ as a failure coefficient, it can be calculated as:

$$\theta=\left(\gamma_m\gamma_{SC}\frac{M}{\alpha_c M_p}+\left(\frac{\gamma_m\gamma_{SC}P}{\alpha_c S_p}\right)^2\right)^2+\left(\alpha_p\frac{p_i-p_e}{\alpha_c p_b}\right)^2 \quad (4)$$

4. Verification

The same pipeline in Rathbone et al.[23] is selected to verify the proposed finite element model. The pipeline section properties, i.e., outside diameter and thickness, are equal to 508 mm and 23.1 mm, respectively. The geometric shape of the pipeline is shown in Figure 5. The axial compressive force of the pipelines with $\theta =$

4° and $\theta = 2°$ are calculated in this section. It is important to know that the main difference between the present study and Rathbone et al.[23] is that the work introduced here is done in a 3D environment whereas Rathbone et al.'s study in a 2D environment.

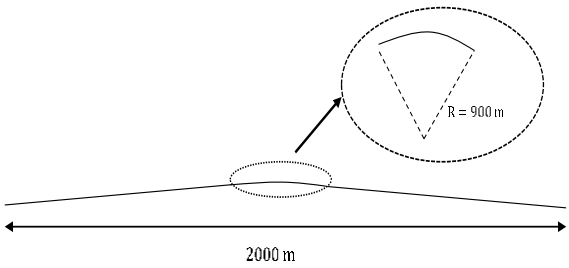

Figure 5. The geometric shape of pipeline

Figure 6 shows the relationship between the axial compressive force and the value of displacement in the midpoint of the pipeline. The peak point of the curve shows the value of the buckle initiation force. Before this point, the pre-buckling stage happens and it can be seen that the axial compressive force increases with small variations in displacement. After the compressive force touches the peak point, the post buckling stage happens and it decreases quickly. As shown in Figure 6, the buckle initiation forces with $\theta = 4°$ and $\theta = 2°$ are 1.71 MN and 1.91 MN, respectively. The critical buckling forces in Rathbone et al. are 1.738 MN and 1.966 MN and the relative error are 2.8% and 5.6% , respectively. Therefore, the proposed finite element model in this research can reach the true critical buckling force of snaked-lay pipelines.

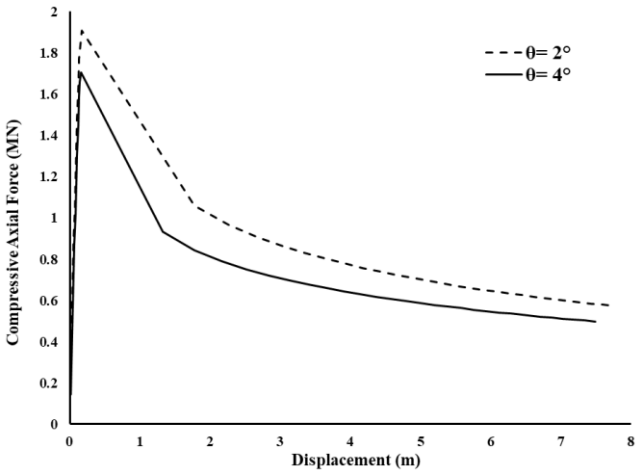

Figure 6. The axial compressive force versus the midpoint pipeline buckling amplitude

5. Factors Influencing the Lateral Buckling

In this paper, it is aimed to investigate the effect of some parameters on the post buckling behavior of pipelines which experience lateral buckling. These parameters include: laying radius (R), offset angle (θ) and laying wavelength (L). The impact of these factors is revealed in the following analyses.

5.1. The Influence of Lay Radius

One of the important parameters which determine the curved section of snaked lay geometry is laying radius. To reveal the influence of the lay radius on the global buckling, pipeline with different values of R is simulated. It must be mentioned that the values of offset angle and laying wavelength are considered 3.38° and 1000 m. In this study, four different values of laying radius, i.e. $200m, 462.5m, 681.25m,$ and $900m$ are considered.

Figure 7 illustrates the resulting buckle shape from a full non-linear FE analysis.

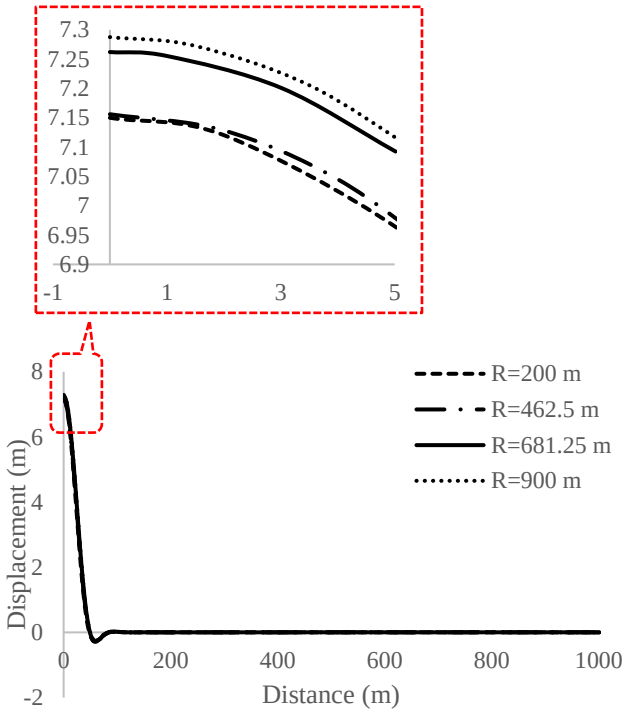

Figure 7. The buckle shape with different laying radiuses

It can be seen that about 90 m of the investigated pipeline experienced displacement and its value grew with the increase in laying radius. The reason of these changes can be explained as follows that by increasing radius, pipeline will deflect more from its straight shape, so this can cause pipeline to deform more easily. The maximum difference in displacement by changing laying radius is about 14% which is occurred in peak point of displacement curve. According to the lateral buckling mode shapes proposed by Hobbs [6], it is obvious that this pipeline is in mode 3. It should be noted that, this figure displays the lateral displacement of a quarter of the pipeline starting from point zero on the horizontal axis.

Effect of laying radius changings on the bending moment and axial force in post buckling stage are shown in Figures 8 and 9.

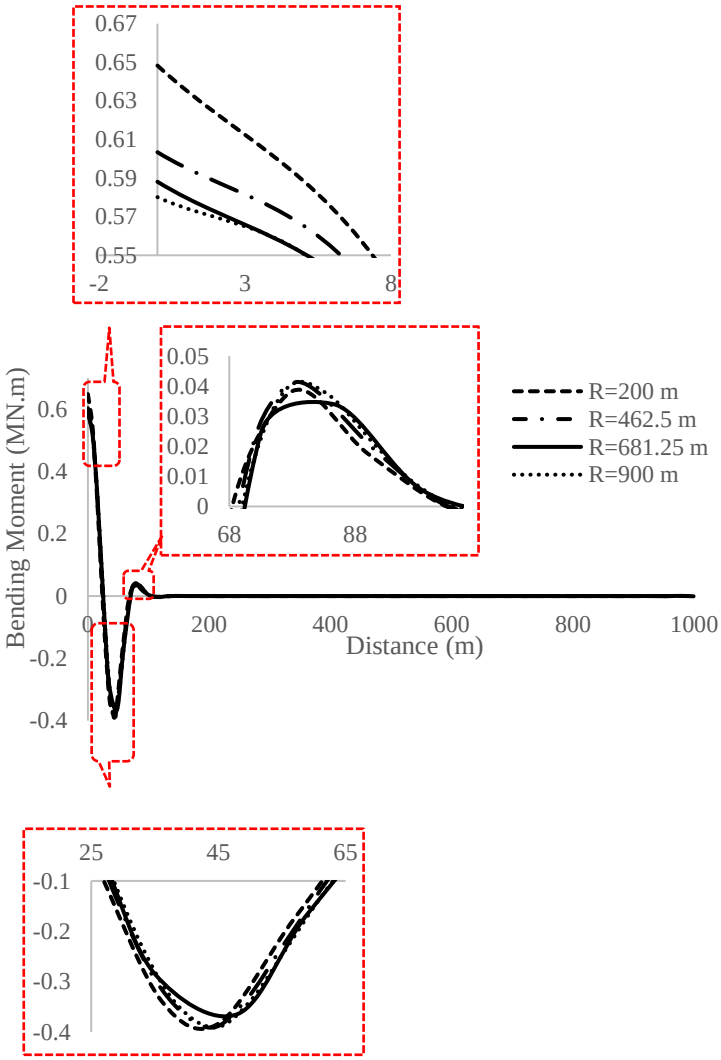

Figure 8. The bending moment of pipelines with different laying radiuses

In order to show more details of curves in some critical regions, some figures are added to the main curve which are displaced in dash line squares and zoomed on some selected regions. As it is observed, the maximum value of bending moment is happened in middle of pipeline and then after $100m$, this value become constant and it is near zero. It is markworthy to know that bending moment is decreased by increasing laying radius. There are similarities in general form of bending moment (Figure 8) and displacement curve (Figure 7), but the rate of changes is contrary. By comparison the maximum value of bending, it is concluded that maximum difference is about 68% and it is happened between $R = 900\ m$ and $R = 200m$.

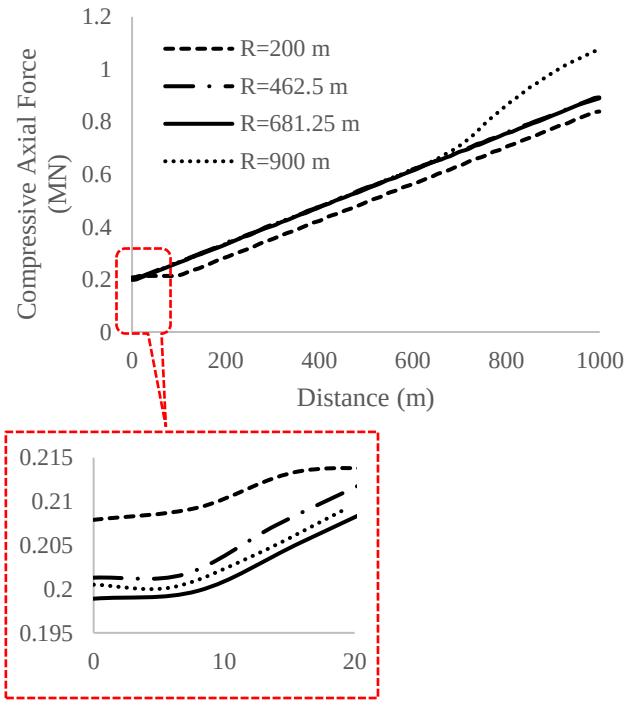

Figure 9. The axial force of pipelines with different laying radiuses

By investigating Figure 9, it is obvious that by moving away from the middle of pipeline, axial force is increased and, in each case, the maximum value is occurred at the constrained end of pipe, because axial movement of pipeline is occurred toward the middle of pipeline and since the friction force is in opposite direction of pipeline movement, so its effect is added to compressive axial force of middle of pipeline and it cause that axial force increase gradually in pipeline length. The axial and frictional force distributions are shown in Figure 10 and 11. The rate of changes of axial force in middle and end of pipeline is different. In general, in middle of pipeline the value of axial force is decreased by increasing R but at the end of pipeline, it is increased by increasing R. The maximum difference of changes is happened at the end of pipeline and it is about 23.1% which occurs between $R = 900\ m$ and $R = 200\ m$. By knowing this, now it is easier to explain the reason of changes of bending moment in Figure 8. Since bending moment is result of lateral and axial forces which have some distance to a fixed point, so larger force will cause larger bending moment which will become more obvious by comparing Figures 8 and 9.

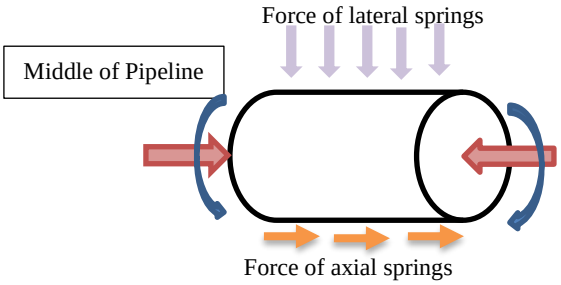

Figure 10. Axial forces on pipeline with positive displacement

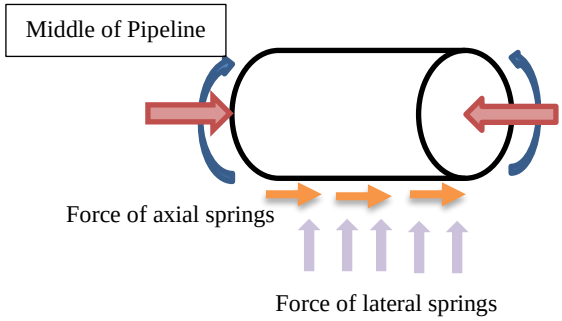

Figure 11. Axial forces on pipeline with negative displacement

The global buckling failure assessment is based on the internal force combination; so, the axial force and bending moment for two cross-sections A and B are used to investigate the global buckling failure. Cross-section A is the cross-section of middle part of pipeline which has the maximum value of bending moment and minimum value of axial force, cross-section B is the end part of pipeline which has maximum value of axial force and minimum value of bending moment. The largest one between θ_A represent the state of cross-section A and θ_B represent the state of cross-section B, which is chosen to assess the post-pipeline's state. The calculation results are shown in Table 3. As it is observed, the failure coefficient is decreased about 11% by increasing laying radius from $200m$ to $900\ m$, which means that in lower values of laying radius, there is the possibility of pipeline failure because of global buckling.

5.2. The Influence of Offset Angle

Offset angle is another important parameter in determining the curved section of snake laying configuration. This assessment is done for pipeline with laying radius of $462.5\ m$ and laying wavelength of $1000\ m$, while the value of offset angle is changed from $3.5\,°$ to $9.125\,°$. As it is observed in Figure 11, the value of pipeline displacement is decreased about 64% by increasing offset angle. The reason of these changes can be explained as follows that by decreasing θ, the value of deviation from straight shape is increased and it will provide a better condition for pipeline displacement. In different introduced values of offset angle, pipeline experiences third mode and displacement become zero about $90\ m$ of horizontal distance. The effect of variation of offset angle on axial force and bending moment of pipeline are shown in Figures 13 and 14.

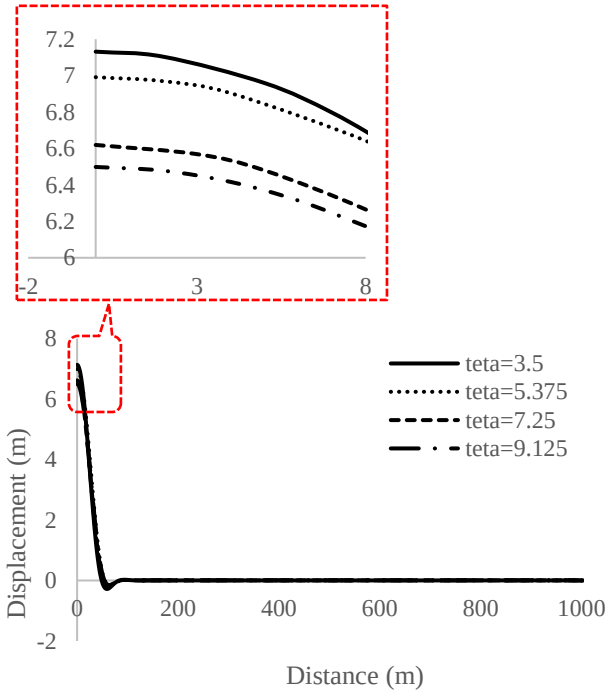

Figure 12. The buckle shape with different offset angles

By investigation of axial force and bending moment curves, it can be concluded that the values of axial force and bending moment are decreased by increasing offset angle and axial force increases linearly with increasing distance from the middle of pipeline. The similarity between changes of bending moment and axial force with changes of offset angle is explained in previous section.

Table 3. global buckling failure assessment by laying radius variation

Laying Radius (m)	Cross-Section	Axial Force (MN)	Bending Moment (N. m)	Failure Coefficient	Larger Failure Coefficient
900	A	0.201	0.58 e6	0.455	0.455
	B	0.107	-0.506 e3	0.417 e-5	
681.25	A	0.199	0.588 e6	0.467	0.467
	B	0.89	-0.814 e3	2.02 e-4	
462.5	A	0.201	0.603 e6	0.491	0.491
	B	0.893	-0.742 e3	2.02 e-4	
200	A	0.208	0.648 e6	0.567	0.567
	B	0.839	-0.628 e3	1.57 e-4	

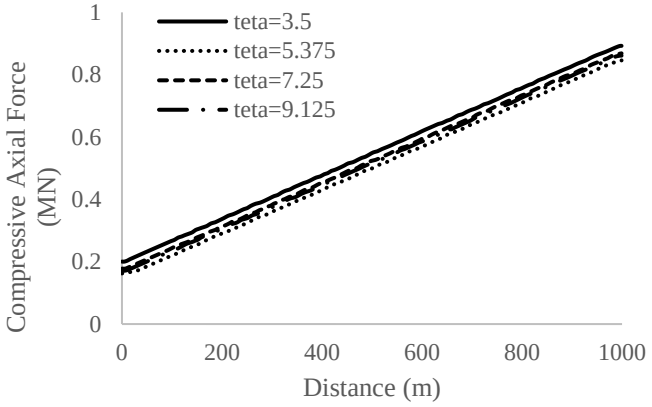

Figure 12. The axial force for pipeline with different offset angles

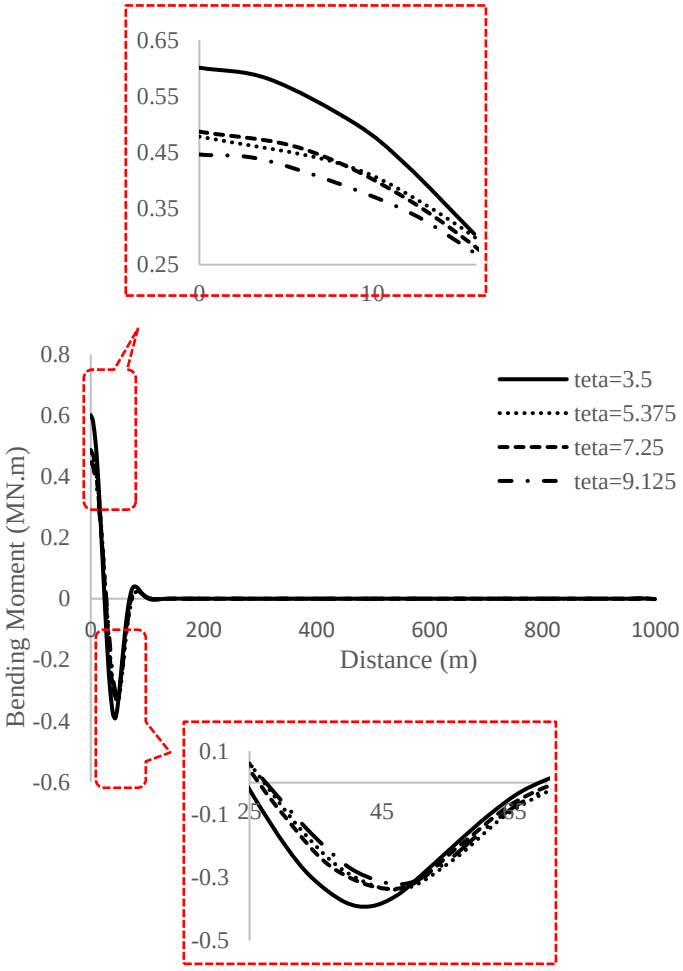

Figure 13. The bending moment for pipeline with different offset angles

The maximum difference of bending moment and axial force are about 155% and 30%. As it is observed in Figure 13, by increasing offset angle, the value of bending moment becomes constant after $100\,m$. By comparing values of failure coefficient, it is concluded that possibility of failure is decreased by increasing offset angle and global buckling failure will not occur because the largest failure coefficient is less than 1. The maximum difference in this range of offset angle is about 21.9 %.

5.3. The Influence of Laying Wave Length

Laying wave length determines the overall length of laid pipeline on seabed. In this study, a pipeline with laying radius of $462.5\,m$ and offset angle of 3.5° is considered and the value of one quarter of laying wavelength is changed between $700\,m$ and $1000\,m$. As it is observed in Figure 14, in different values of laying wavelengths, pipeline is in third mode and the value of displacement is increased by increasing wavelength because larger region of pipeline is free to move and the middle of pipeline is far away from constrained sections. Investigation of introduced curve shows that about $90\,m$ of pipeline will experience displacement and after that it becomes about zero. Maximum difference in this curve is on the peak point of displacement and it is about 133.6%. The effect of variation of laying wavelength on axial force and bending moment of pipeline are shown in Figures 15 and 16.

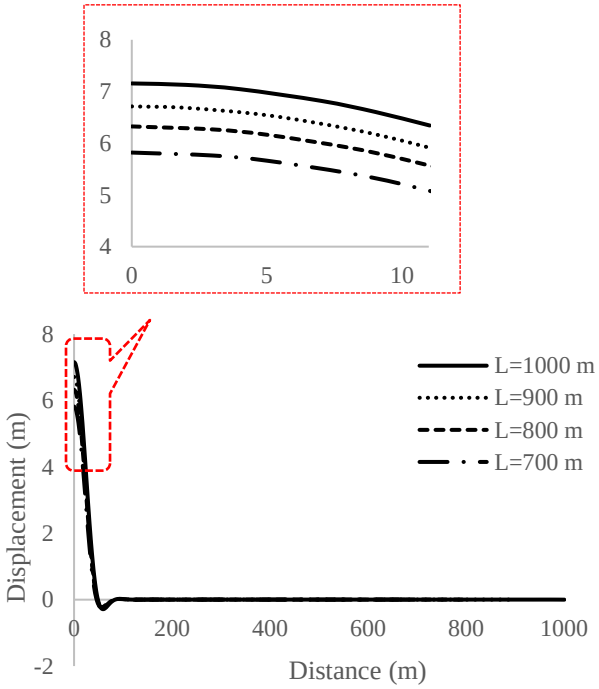

Figure 14. The buckle shape with different laying wavelengths

Comparison of axial force curves and bending moment curves of Figures 15 and 16 shows that bending moment is increased by increasing laying wavelength but the axial force will be decreased. The axial force increases linearly with increasing distance from the middle of pipeline and the reason of changes are explained in section 5.1 and like previous figures, there are similarities in appearance of displacement and bending moment curve.

Table 4. global buckling failure assessment by offset angle variation

Offset Angle (°)	Cross-Section	Axial Force (MN)	Bending Moment (N. m)	Failure Coefficient	Larger Failure Coefficient
9.125	A	0.171	0.446 e6	0.269	0.269
	B	0.861	-2.06 e3	2.19 e-4	
7.25	A	0.178	0.487 e6	0.32	0.32
	B	0.869	-1.6 e3	2.1 e-4	
5.375	A	0.163	0.478 e6	0.309	0.309
	B	0.846	-1.08 e3	1.76 e-4	
3.5	A	0.201	0.601 e6	0.488	0.488
	B	0.893	-0.912 e3	2.07 e-4	

The reason of changes of curves 15 and 16 with laying wave length is explained in the following. By referring to Figure 15, it is obvious that by decreasing length of pipeline, the length of free region and the value of deviation from straight form will decrease and the resistance against axial movement of pipeline will increase which will cause larger values of axial force. In order to analyze Figure 16, it is important to know that the rate of changes of bending moment is depend on axial force and lateral force which the second is exerted by lateral springs and according to Table 2, in large values of displacement, lateral force is constant. So, by getting away from the pipeline end, the effect of lateral force is added to each segment and by increasing pipeline length, more of this effect will added, so it will cause larger bending moment in larger values of pipeline length.

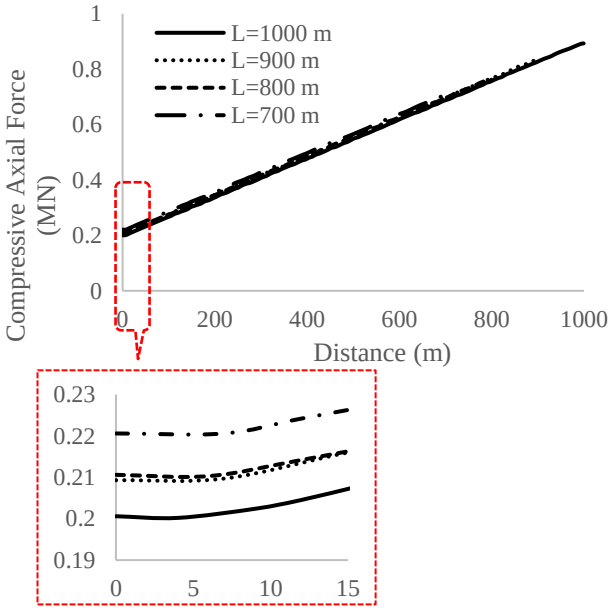

Figure 15. The axial force for pipeline with different laying wavelengths

Maximum difference in bending moment and axial force is about 54% and 20%. As it is observed in Figure 16, by increasing offset angle, the value of bending moment becomes constant after 100 m.
Investigation of Table 5 shows that the largest value of failure coefficient is occurred in laying wavelength of $1000\,m$ and its value decreased by increasing laying wavelength. The maximum difference is 8.3%.

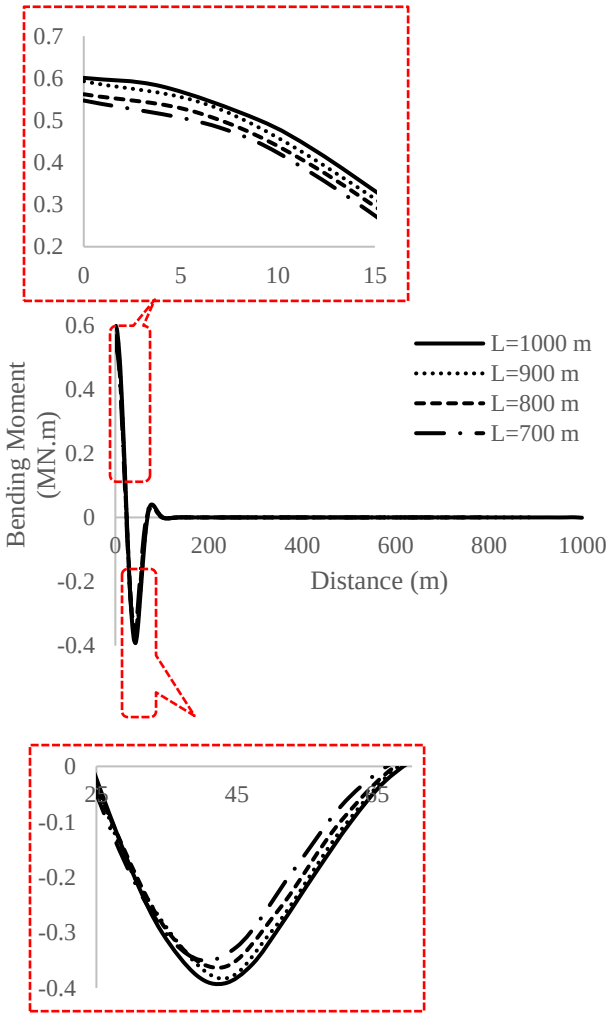

Figure 16. The bending moment for pipeline with different laying wavelengths

6. Conclusions

In this study, the numerical simulation method is employed to calculate the lateral deformation of snaked lay pipelines under HP/HT condition. According to global buckling failure assessment recommended in the DNV code, the influences of laying wavelength, laying radius and offset angle on global buckling failure are analyzed. The main conclusions are as follow:
1. A pipeline with constant loading and cross section but different configurations are heated and pressured.

Table 5. Global buckling failure assessment by laying wave length variation

Laying wavelength (m)	Cross-Section	Axial Force (MN)	Bending Moment (N. m)	Failure Coefficient	Larger Failure Coefficient
2000	A	0.201	0.601 e6	0.488	0.488
	B	0.893	-0.912 e3	2.07 e-4	
1800	A	0.209	0.593 e6	0.475	0.475
	B	0.832	-0.488 e3	1.48 e-4	
1600	A	0.211	0.562 e6	0.427	0.427
	B	0.762	-0.868 e3	1.17 e-4	
1400	A	0.221	0.547 e6	0.405	0.405
	B	0.702	-0.64 e3	8.3 e-5	

Investigation of changing of laying radius, offset angle and laying wavelength, which are the main parameters in determination of snake lay configuration, shows that:

a. By increasing offset angle, values of bending moment, axial force and displacement will decrease and maximum difference is related to bending moment which is about 155%.

b. By increasing laying radius, the value of bending moment is decreased but the values of axial force and displacement will increase and maximum difference is related to bending moment which is about 68%.

c. By increasing laying wavelength, the value of axial force decreased but the values of bending moment and displacement will increase and maximum difference is related to displacement which is about133.6%.

2. Post- buckling pipeline failure state is also checked. Two critical cross section are chosen and assessed. Results show that the cross-section A is the most critical region in snaked lay pipelines.

3. Effect of three parameters, i.e., offset angle, laying radius and laying wavelength of global buckling failure of pipelines are investigated and results showed that by decreasing offset angle and laying radius, failure coefficient is increased. Since the values of offset angle and laying radius determine the curve section of snake lay configuration, it can be concluded that as the curved section shrinks, the possibility of global buckling failure will increase. But the effect of laying wavelength is opposite and by decreasing the laying wavelength, failure coefficient will decrease about 8.3%.

7. References

1- GUO, L.-P., LIU, R. and YAN, S.-W.,(2013), *Global buckling behavior of submarine unburied pipelines under thermal stress*, Journal of central south university, 20(7), p. 2054-2065.

2- CHEUK, C., WHITE, D. and BOLTON, M.,(2005), in *Proceedings of the International Conference on Soil Mechanics and Geotechnical Engineering*.

3- 2007), in *DNV-RP-F110*. Hovik, Norway.

4- RUNDSAG, J. O., TØRNES, K., CUMMING, G., RATHBONE, A. D. and ROBERTS, C.,(2008), in *Eighteenth International Offshore and Polar Engineering Conference*. International Society of Offshore and Polar Engineers.

5- WANG, Z. and TANG, Y.,(2020), *Antisymmetric thermal buckling triggered by dual distributed buoyancy sections*, Marine Structures, 74, p. 102811.

6- HOBBS, R. E.,(1984), *In-service buckling of heated pipelines*, Journal of Transportation Engineering., 110(2), p. 175-189.

7- TAYLOR, N. and GAN, A. B.,(1986), *Submarine pipeline buckling—imperfection studies*, Thin-Walled Structures, 4(4), p. 295-323.

8- HONG, Z., LIU, R., LIU, W. and YAN, S.,(2015), *Study on lateral buckling characteristics of a submarine pipeline with a single arch symmetric initial imperfection*, Ocean engineering, 108, p. 21-32.

9- TIANFENG, Z. and XIANHONG, F.,(2015), *Upheaval buckling solution for submarine pipelines by segmented ditching and hot water flushing*, Ocean engineering, 102, p. 129-135.

10- WANG, Z., VAN DER HEIJDEN, G. and TANG, Y.,(2018), *Analytical study of third-mode lateral thermal buckling for unburied subsea pipelines with sleeper*, Engineering Structures, 168, p. 447-461.

11- WANG, Z., TANG, Y. and WANG, C.,(2017), *Analytical solution for lateral buckling of unburied subsea pipelines with distributed buoyancy section*, Ocean engineering, 146, p. 115-124.

12- WANG, Z., TANG, Y., ZHOU, L., ZHAO, Z. and WANG, C.,(2017), *Analytical solution for controlled lateral buckling of unburied subsea pipelines*, Ocean engineering, 146, p. 140-150.

13- WANG, L., SHI, R., YUAN, F., GUO, Z. and YU, L.,(2011), *Global buckling of pipelines in the vertical plane with a soft seabed*, Applied Ocean Research, 33(2), p. 130-136.

14- SHI, R., WANG, L., GUO, Z. and YUAN, F.,(2013), *Upheaval buckling of a pipeline*

with prop imperfection on a plastic soft seabed, Thin-Walled Structures, 65, p. 1-6.

15- SHI, R. and WANG, L.,(2015), *Single buoyancy load to trigger lateral buckles in pipelines on a soft seabed*, Journal of Engineering Mechanics, 141(5), p. 04014151.

16- WANG, Z., CHEN, Z., HE, Y. and LIU, H.,(2015), in *The Twenty-fifth International Ocean and Polar Engineering Conference*. International Society of Offshore and Polar Engineers.

17- LI, Z.-G., WANG, C., HE, N. and ZHAO, D.-Y.,(2008), *An overview of deepwater pipeline laying technology*, China Ocean Engineering, 22(3), p. 521-532.

18- LIU, W. and FU, J.,(2018), in *The 28th International Ocean and Polar Engineering Conference*. International Society of Offshore and Polar Engineers.

19- GUAN, J., NYSTRØM, P. R. and HANSEN, H. F.,(2007), in *International Conference on Offshore Mechanics and Arctic Engineering*. vol. 4269, p. 219-227.

20- MATHESON, I., CARR, M., PEEK, R., SAUNDERS, P. and GEORGE, N.,(2008), in *ASME 2004 23rd International Conference on Offshore Mechanics and Arctic Engineering*. American Society of Mechanical Engineers Digital Collection, p. 67-76.

21- WAGSTAFF, M.,(2003), in *Proceedings of the Petromin Pipeline Conference, Singapore*.

22- PRESTON, R., DRENNAN, F. and CAMERON, C.,(1999), in *The Ninth International Offshore and Polar Engineering Conference*. International Society of Offshore and Polar Engineers.

23- RATHBONE, A., TØRNES, K., CUMMING, G., ROBERTS, C. and RUNDSAG, J.,(2008), in *The Eighteenth International Offshore and Polar Engineering Conference*. International Society of Offshore and Polar Engineers.

24- G. CUMMING and RATHBONE, A.,(2010), in *ASME 2010 International conference on ocean, offshore and arctic engineering*.

25- OBELE, I., (2013), Lateral buckling and axial walking of surface laid subsea pipeline, University of Stavanger, Norway. p.

26- REZAIE, Y., SHARIFI, M. H., RASHED, G. and NUMANI, F.,(2020), *A parametric study of critical buckling force in snaked lay pipelines under HP/HT condition*, International Journal of Coastal and Offshore Engineering, 4, p. 49-56.

27- LIU, Y., LI, X. and ZHOU, J.,(2013), *Post-buckling studies on snaked-lay pipeline with new shape*, Journal of information & computational science, 9(12), p. 3315-3324.

28- KARAMPOUR, H., ALBERMANI, F. and GROSS, J.,(2013), *On lateral and upheaval buckling of subsea pipelines*, Engineering Structures, 52, p. 317-330.

29- 2010), in *DNV-OS-F101*. Hovik, Norway.

30- ZHANG, Y., YI, D., XIAO, Z. and HUANG, Z.,(2015), *Engineering critical assessment for offshore pipelines with 3-D elliptical embedded cracks*, Engineering Failure Analysis, 51(1), p. 37-54.

31- HIBBITT , KARLSSON and SORENSEN, (2013), *ABAQUS/STANDARD. User's Guide and Theoretical Manual, Version 6.13*.

32- HONG, Z., LIU, R., LIU, W. and YAN, S.,(2015), *A lateral global buckling failure envelope for a high temperature and high pressure (HT/HP) submarine pipeline*, Applied Ocean Research, 51, p. 117-128.